COMMUNICATION

Organic Electrochemical Transistors with Maximum Transconductance at Zero Gate Bias

*Jonathan Rivnay, Pierre Leleux, Michele Sessolo, Dion Khodagholy, Thierry Hervé, Michel Fiocchi, and George G. Malliaras**

As lab-on-chip platforms for biomedical applications become more sophisticated by increasing the number of fluidic, electronic, and/or mechanical components, space and design restrictions become more stringent.[1] Organic transistors provide unique opportunities when integrated into these systems as transducers that can be easily patterned, individually functionalized, and directly interfaced with biomolecules and living cells.[2] Inherently, transistor operation involves the application of a bias, V_g, between source and gate, and a separate bias, V_d, between source and drain, and hence requires two power supplies. Making available two voltage connections to each transistor renders these devices challenging to implement on a chip that contains numerous other components. In principle, a circuit could be built that provides both gate and drain bias from a single supply, but this is a costly solution in terms of real estate on the chip. Moreover, minimizing V_g is important when biorecognition elements such as bilayer membranes and cells are used, as these can be sensitive to prolonged application of a bias.[3] To this end, we engineer an organic electrochemical transistor (OECT) with its maximum transconductance at zero applied gate bias. By carefully selecting device geometry and operating conditions, a micron-scale transistor with a high transconductance (≈2 mS) is presented which can act as an amplifying transducer for detecting minute electrical potentials, biased with just one power supply. A simple amplifier with a voltage gain of 12 and a large power gain is demonstrated. This paves the way for new designs of biosensor devices in which amplification is achieved by a transducer with improved operational simplicity.

Organic electrochemical transistors (OECTs) offer a unique set of advantages in the development of biomedical tools. Compared to traditional field-effect transistors, which require an oxide layer with precisely controlled thickness between the channel and the gate, OECTs are simple to fabricate. They consist of a conducting polymer channel in direct contact with an electrolyte, in which a gate electrode is immersed.[4] In addition to their ease of solution processing, synthetic freedom for (bio-) functionalization, and their ability to take on unique form factors,[5] OECTs allow for direct interfacing of the active material with an analyte or biological environment.[6] They have been employed as environmental and biochemical sensors,[7,8] interfaced with cell cultures to control cell adhesion,[9] monitor cell viability,[10] and barrier tissue integrity,[11] and used in vivo to record brain activity.[12] In most of these cases, the OECTs are employed as amplifying transducers, and more specifically as transconductance amplifiers: a biological event modulates the effective gate bias, which changes the drain current, I_d. This configuration amplifies the power of an input signal at the gate by a factor that is determined by the transistor's transconductance, $g_m = \Delta I_d / \Delta V_g$. This was recently demonstrated by Khodagholy, et al.,[12] who showed that OECTs outperform electrodes in recording local field potentials arising from neurons in the brain due to local signal amplification.

Electrochemical transistors based on conducting polymers, such as the one initially reported by White, et al.[13] utilizing polypyrrole, and more recently those based on poly(3,4-ethylenedioxythiophene) poly(styrenesulfonate) (PEDOT:PSS),[4,7] operate in depletion mode. In the latter, for example, the active material is composed of a polymeric semiconductor, PEDOT, which is doped p-type by the sulfonate groups of the polyanion PSS, making the complex PEDOT:PSS highly conducting.[14] As a result, an unbiased PEDOT:PSS OECT channel is effectively "ON". Upon application of a positive gate bias, cations from the electrolyte (an aqueous salt solution in our case) are injected into the conducting polymer channel, compensating the sulfonate groups on the PSS, thereby de-doping the PEDOT. This increases the channel resistance, bringing the transistor to the "OFF" state. Ion penetration into the channel is therefore the identifying characteristic of OECTs, resulting in an operation mechanism that is distinctly different than that of organic field-effect transistors (OFETs).[15] Tuning the transfer characteristics OFETs has been extensively studied and can be accomplished, for example, by modifying dopant and/or trap density and by using different gate electrode materials.[16,17] Given the inherently different operating mechanism of OECTs, however, engineering the transfer characteristics is not as well understood, and is thus the focus of the present work.

We used photolithography to define OECTs with channel dimensions of 100 μm and below (**Figure 1**). Arrays of transistors were fabricated by patterning Au source and drain electrodes and interconnects on glass substrates. The interconnects were insulated from the aqueous electrolyte by a vapor-polymerized parylene-C layer. The active PEDOT:PSS channel

Dr. J. Rivnay, P. Leleux, Dr. M. Sessolo,
Dr. D. Khodagholy, M. Fiocchi, Prof. G. G. Malliaras
Department of Bioelectronics
Ecole Nationale Supérieure des Mines
CMP-EMSE, MOC, 880 route de Mimet
13541, Gardanne, France
E-mail: malliaras@emse.fr
P. Leleux, Dr. T. Hervé
Microvitae Technologies
Pole d'Activite Y. Morandat, 13120, Gardanne, France

DOI: 10.1002/adma.201303080

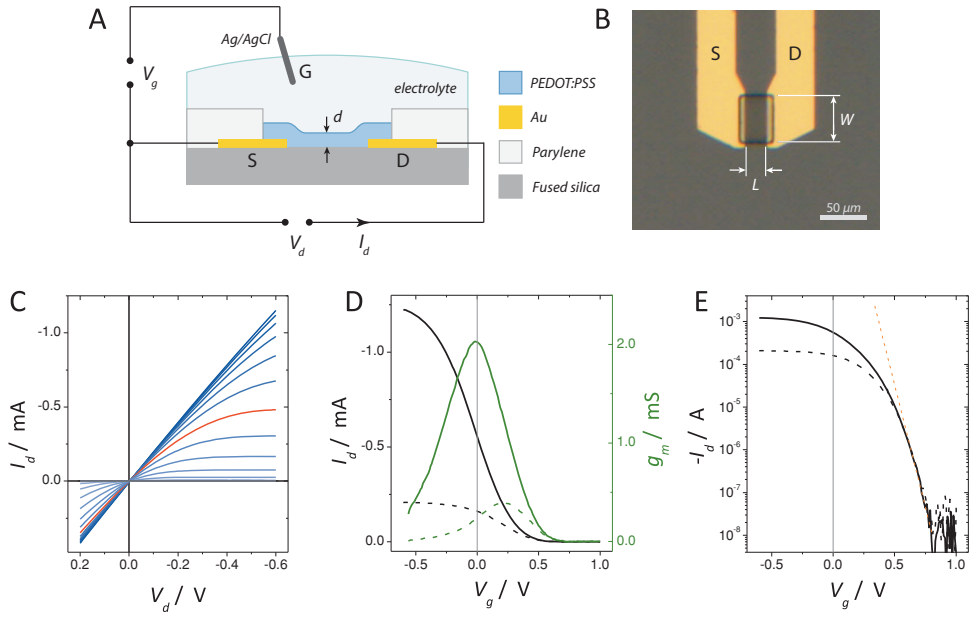

Figure 1. High performance organic electrochemical transistors (OECT) with maximum transconductance at zero gate bias. (A) Cross section schematic and wiring of an OECT, and (B) micrograph of a typical device showing device architecture. (C) Output characteristics of a device (W/L = 10 µm/5 µm, d = 140 nm) from V_g = –0.6 V (top) to 1 V. The curve for V_g = 0 V is highlighted in red. (D) Transfer characteristics and resulting transconductance at V_d = –0.6 V (solid line) and V_d = –0.1 V (dashed line). (E). Transfer characteristics on a log scale (indicating subthreshold slope, dotted line).

(deposited from a commercially available dispersion) and the insulating parylene layer were simultaneously patterned using a second sacrificial parylene layer, as detailed in the Experimental Section. The resulting device geometry is shown in Figures 1A,B, whereby the channel width (W) and length (L) was photolithographically defined, and channel thickness (d) was determined by the spin casting conditions and number of layers deposited. Devices were operated in the common source configuration with a 100 mM NaCl water solution in direct contact with the conducting polymer. The gate electrode, in this case a Ag/AgCl pellet, was immersed in the electrolyte.

The transistor characteristics were evaluated from a series of gate and drain bias sweeps while monitoring the drain current. The output characteristics of an OECT with W = 10 µm, L = 5 µm, and d ~ 140 nm (Figure 1C) show the low voltage operation typical of electrolyte-gated transistors.[7,15] A positive gate bias de-dopes the channel and decreases the absolute value of the current. The corresponding transfer curve (Figure 1D) shows that at a drain voltage of –0.6 V, the drain current exceeds 1 mA. More importantly, the transconductance is shown to exhibit its maximum value of $g_{m,max}$≈2 mS at V_g = 0 V. The device geometry used to attain these characteristics resulted in a number of other advantageous outcomes: the relatively small channel volume allowed for the PEDOT:PSS channel to be completely shut off at gate biases <1 V (0.8 V in Figure 1E), which to the best of our knowledge has not been achieved previously for an OECT. Consequently, the device exhibits an ON/OFF current ratio ≈10^5, and a subthreshold slope of 75 mV dec^{-1}.

To be able to engineer the device with a maximum transconductance at zero gate voltage shown in Figure 1, we explored the scaling of the transfer curves with channel geometry. The gate bias at which the maximum transconductance is reached, $V_g(g_{m,max})$, was found to exhibit a strong dependence on W/L, as well as on channel thickness (**Figure 2**). Varying the aspect ratio of the channel while keeping channel thickness constant shows that a larger W/L results in a higher maximum transconductance. More importantly, a larger gate bias must be applied in order to achieve the maximum transconductance. For example, a difference in $V_g(g_{m,max})$ of +0.3 V is seen between devices with a W/L of 0.1 and of 10. At the same time, thicker active channels result in both higher $g_{m,max}$, as well as higher $V_g(g_{m,max})$ values. Changing the thickness of the PEDOT:PSS channel from 25 to 640 nm increases $V_g(g_{m,max})$ by +0.3 V. The conducting polymer channel dimensions therefore represent an effective route to tune the gate bias at which the maximum transconductance is achieved. Over the thickness and channel size scales explored in this work, an overall variation of ≈0.6 V is achieved, which is significant for a device with such low voltage operation. It should be noted that $V_g(g_{m,max})$ is independent of device area, as long as the ratio W/L and the channel thickness remain the same (Supporting Information, Figure S1).

The shape of the transconductance vs. gate bias curve can be described by understanding the limits of OECT device operation. Above a certain applied positive gate bias (>0.75 V in Figure 1D) the transistor reaches the OFF state in which part of the channel is completely de-doped, and hence the drain current is very low (<10 nA). Increasing the gate bias any further does not change the drain current appreciably and hence the transconductance approaches zero. At the other extreme, application of a sufficiently high negative gate bias turns the transistor to its ON state, where the channel is fully doped. A further decrease of the gate bias does not increase the drain

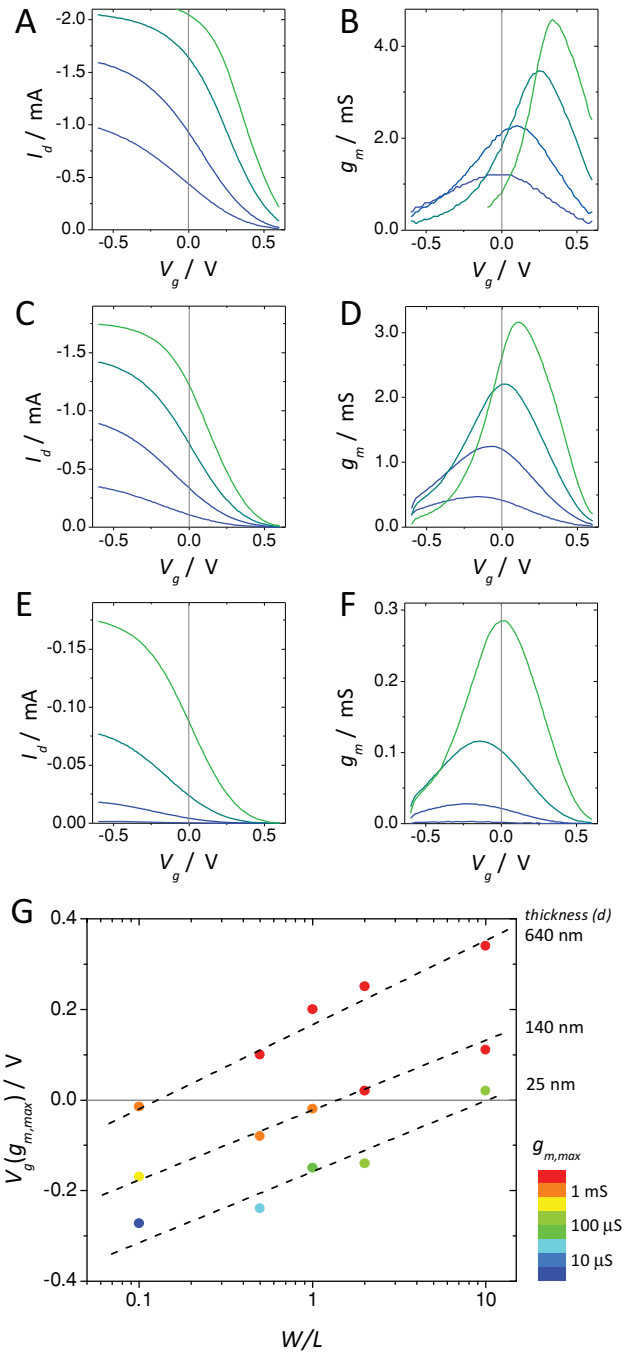

Figure 2. Engineering maximum transconductance at V_g = 0 V by geometrical scaling (W/L, thickness). Transfer curves (A,C,E), and transconductance (B,D,F) of OECTs with PEDOT:PSS thickness of 640 nm (A,B), 140 nm (C,D), and 25 nm (E,F). For each plot, channel geometry is varied: W(µm)/L(µm) = 100/10, 50/25, 25/50, 10/100 from green to blue (top to bottom). (G) V_g required to achieve maximum transconductance, as a function of W/L for different channel thicknesses. Values are color coded according to maximum transconductance value. Dashed lines are guides to the eye.

current. Thus, at sufficiently positive and negative gate bias, the transconductance approaches zero, and reaches a maximum at an intermediate value. An inspection of the transfer curves in Figures 2A-C shows that as W/L increases, so does the ON current. As a result, $V_g(g_{m,max})$ shifts to higher values. Moreover, the transfer curves show that V_{ON} (the gate bias required to begin turning the transistor ON when sweeping from positive gate bias), does not vary significantly with W/L (Figure S2). This finding suggests that pinch-off occurs and only part of the channel is de-doped.[4]

In addition to changing channel geometry, $V_g(g_{m,max})$ can be tuned through the use of a different gate electrode materials. As in the case of electrolyte-gated field effect transistors,[17] we found that different gate electrode materials shift the transfer curve in a way that reflects the voltage drop at the gate/electrolyte interface (Figures S3, S4). Ag/AgCl, being a non-polarizable electrode, is the most effective at turning the transistor OFF, while a larger gate bias needs to be applied to Pt, a polarizable electrode, to achieve the same effect.[18] PEDOT:PSS falls in between these two cases, though it should be noted that the three gate electrodes did not have the exact same area, and hence a quantitative comparison cannot be made. For a practical application, the choice of gate electrode material will be dictated by the need for biofunctionalization and the constraints of the fabrication process. For a particular gate electrode, therefore, channel geometry can be optimized in order to yield $g_{m,max}$ at zero gate bias. It should be noted that $V_g(g_{m,max})$ bears a slight dependence on the applied drain bias (Figure 1D). Typically, $V_g(g_{m,max})$ shifts by 250 mV over the applied range of drain bias explored here. However, $g_{m,max}$ decreases significantly as V_d is lowered and as a result decreasing the drain bias does not represent a promising avenue to tune device characteristics.

The transistor performance trends shown in Figure 2G reveal that a $V_g(g_{m,max})$ = 0 V can be achieved by selecting a number of channel dimension combinations: for example, small W/L for thick channels or large W/L for thin ones. However, a number of tradeoffs are important in choosing the appropriate geometry. In many cases, high transconductance and compact size are often simultaneously desirable. In addition, it has been shown that OECTs with micron-scale channels are capable of a fast response (with time constants below 100 µs), sufficiently fast for capturing neural activity.[19] Thus, high transconductance in a compact device that shows a fast response time, while having $V_g(g_{m,max})$ = 0 V, can be achieved with an OECT with channel dimensions of L = 5 µm, d = 140 nm, and $W/L \approx$ 1–2. These are the dimensions of the OECT whose transfer curve is shown in Figure 1D.

A simple transducer circuit one could build with an OECT is a voltage amplifier. Such a circuit is shown in the diagram in the inset of **Figure 3**, in which the channel is connected to a battery through a series resistor, across which the output voltage is measured. A gate electrode, immersed in the electrolyte, is directly connected to the source without a DC bias. In this configuration, an event in the electrolyte that causes a change in the potential across the gate/electrolyte or electrolyte/channel interface (e.g., an enzymatic reaction)[20] is manifested as a voltage change across the drain resistor. We simulated such an event by introducing a small oscillatory signal at the gate with an amplitude ΔV_g = 10 mV and measured the amplitude of modulation ΔV_R of the output voltage over the resistor R_L = 10 kΩ. The value of the resistor was selected so as to bring the OECT to the maximum transconductance point. The voltage

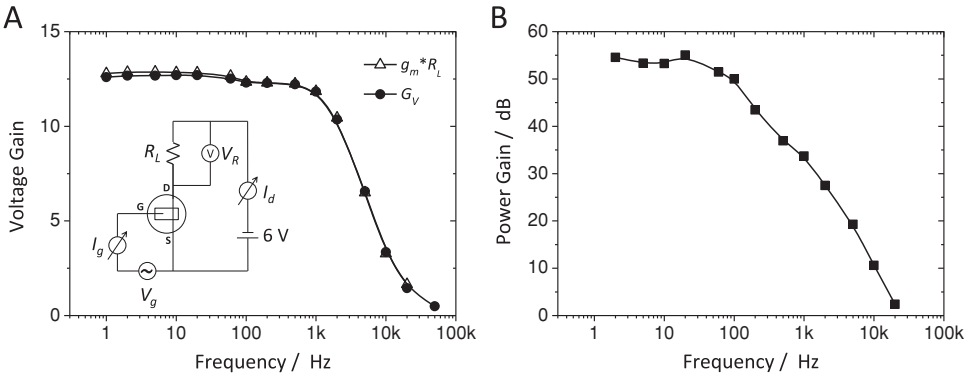

Figure 3. Small-signal response of the amplifier circuit (inset) using an OECT (W/L = 10 µm/10 µm, 120 nm thick, $g_{m,max} \approx 1.5$ mS), and a drain resistor, R_L = 10 kΩ as a function of frequency. (A) voltage gain of the circuit in response to a 10 mV amplitude modulation at the gate. The gate bias offset was zero. Voltage gain calculated from the transconductance of the OECT multiplied by R_L is also shown. (B) Corresponding power gain in dB as a function of frequency.

gain, $G_V = \Delta V_R / \Delta V_g$, is shown as filled circles in Figure 3A to be ≈12 up to a frequency of 1 kHz, a cut-off consistent with our previous work on micron-scale OECTs.[12] One can show that the expected voltage gain in this amplifier is equal to the product $g_m \cdot R_L$. We thus measured the transconductance of the OECT itself as a function of frequency and calculated the product $g_m \cdot R_L$, shown by open triangles in Figure 3A to be in excellent agreement with the measured gain. It should be mentioned that a gain of 12 represents a high value for such a simple circuit, and comes with the added benefit of linearity, associated with operating at maximum transconductance. A higher voltage gain could be extracted by operating the OECT in the subthreshold regime, but that would require biasing the gate and result in a loss of linearity. The power gain, G_P was calculated from:

$$G_P = 10 \cdot \log \frac{P_{OUT}}{P_{IN}} \quad (1)$$

where P_{IN} and P_{OUT} are the powers of the input and output signals, respectively, defined as:

$$P_{IN} = \frac{1}{2} \Delta V_g \Delta I_g \cos \varphi_{I_g} \quad (2)$$

$$P_{OUT} = \frac{1}{2} \Delta V_R \Delta I_d \cos \left(\varphi_{V_R} - \varphi_{I_d} \right) \quad (3)$$

where ΔI denotes the amplitude of current modulation and φ is the phase shift with respect to the input voltage. The power gain in Figure 3B shows a gradual decrease with frequency, with a low-frequency value of 55 dB. This power gain can be utilized to amplify a signal of biological origin right at the point of transduction, making the measurement much less sensitive to noise arising from wires and circuitry connecting to the acquisition system.

In this work, we demonstrate a micron-scale, high performance organic electrochemical transistor, which exhibits its maximum transconductance at zero applied gate bias. By investigating a variety of device sizes and operating conditions we show that the gate bias required to reach maximum transconductance can be varied most significantly by changing the channel width-to-length ratio and thickness. We demonstrate that gate electrode material and drain bias can also be used to tune transistor characteristics. The results show that the OECT can be used as a simple, amplifying transducer that offers a high power gain and a voltage gain exceeding 10. The inherent simplicity associated with operating a transistor at zero gate bias represents a significant step towards less complex amplifying transducers that offer more facile integration into systems for biomedical applications. In addition to facilitating integration with lab-on-chip platforms, the advancements described herein will improve the reliability of OECT-based sensors that utilize biorecognition elements such as bilayer membranes and cells, and are sensitive to the prolonged application of a high bias.

Experimental Section

Device Fabrication: The fabrication process, similar to that reported previously,[19,21,22] included the deposition and patterning of metal, parylene, and PEDOT:PSS. Glass slides were thoroughly cleaned by sonication in acetone, isopropyl alcohol, and DI water, followed by a drying step and brief oxygen plasma cleaning. Metal pads, interconnects, and source/drain contacts (defining the channel length) were patterned by a lift-off process, using S1813 photoresist, exposed to UV light using a SUSS MBJ4 contact aligner, and developed using MF-26 developer. 5 nm of chromium and 100 nm of gold were subsequently deposited using a metal evaporator, and metal lift-off was carried out in acetone. Metal interconnects and pads were insulated by depositing 2 µm of parylene C using an SCS Labcoater 2, with a 3-(trimethoxysilyl)propyl methacrylate (A-174 Silane) adhesion promoter. A dilute solution of industrial cleaner (Micro-90) was subsequently spin coated to act as an anti-adhesive for a second, sacrificial 2 µm parylene C film, which was used to simultaneously define the active channel area, and to pattern the underlying parylene layer. Samples were subsequently patterned with a 5 µm thick layer of AZ9260 photoresist and AZ developer (AZ Electronic Materials), defining the active channel width, which was exposed to the electrolyte. The patterned areas were opened by reactive ion etching with an O_2 plasma using an Oxford 80 Plasmalab plus. For the preparation of the PEDOT:PSS films, 20 mL of aqueous dispersion (Clevios PH-1000 from Heraeus Holding GmbH) were mixed with ethylene glycol (1 mL), and dodecyl benzene sulfonic acid (DBSA, 50 µL) – additives used to enhance conductivity and film forming properties–and 1 wt%

of (3-glycidyloxypropyl) trimethoxysilane (GOPS), used to crosslink the film for stable operation in aqueous conditions. The resulting dispersion was spin-coated at 600–3000 rpm, depending on the desired thickness, and baked for 90 seconds at 100 °C. The sacrificial parylene layer was peeled-off, the devices were subsequently baked at 140 °C for 1 h, and then immersed and rinsed in DI water to remove excess low molecular weight compounds and the anti-adhesive.

Device Characterization: All characterization was done using a solution of 100 mM NaCl in DI water as the electrolyte and a Ag/AgCl wire (Warner Instruments) as the gate electrode. Alternative testing was performed with a Pt pellet, and PEDOT:PSS (another device on the same substrate) as gate electrodes (see Supporting Information). The *IV*-characteristics of the OECTs were measured with two VA10 transimpedance amplifiers (NPI) and customized Labview software. The power transfer measurement was performed using a National Instruments PXIe-1062Q system. Two NI-PXI-4071 digital multimeters measured drain and gate currents, and a NI-PXI 6289 measured drain and gate voltage. All the measurements were triggered through the built-in PXI architecture. The recorded signals were saved and analyzed using customized LabVIEW software.

Supporting Information

Supporting Information is available from the Wiley Online Library or from the author.

Acknowledgements

This work was supported by Marie Curie Post-doctoral Fellowships (J.R. and M.S.), the Agence Nationale de la Recherche, and the Partner University Fund (a program of French American Cultural Exchange). We are grateful to Prof. Robert Forchheimer (University of Linköping, Sweden) for his help in understanding the amplifier in Figure 3.

Received: July 5, 2013
Published online: October 2, 2013

[1] S. Schumacher, J. Nestler, T. Otto, M. Wegener, E. Ehrentreich-Forster, D. Michel, K. Wunderlich, S. Palzer, K. Sohn, A. Weber, M. Burgard, A. Grzesiak, A. Teichert, A. Brandenburg, B. Koger, J. Albers, E. Nebling, F. F. Bier, *Lab on a Chip* **2012**, *12*, 464.
[2] R. M. Owens, G. G. Malliaras, *MRS Bull.* **2010**, *35*.
[3] K. Benson, S. Cramer, H.-J. Galla, *Fluids and Barriers of the CNS* **2013**, *10*, 1.
[4] D. A. Bernards, G. G. Malliaras, *Adv. Funct. Mater.* **2007**, *17*, 3538.
[5] a) M. Hamedi, R. Forchheimer, O. Inganas, *Nature Mater.* **2007**, *6*, 357; b) G. Mattana, P. Cosseddu, B. Fraboni, G. G. Malliaras, J. P. Hinestroza, A. Bonfiglio, *Org. Electron.* **2011**, *12*, 2033.
[6] P. Lin, F. Yan, *Adv. Mater.* **2012**, *24*, 34.
[7] D. Nilsson, M. Chen, T. Kugler, T. Remonen, M. Armgarth, M. Berggren, *Adv. Mater.* **2002**, *14*, 51.
[8] a) Z.-T. Zhu, J. T. Mabeck, C. Zhu, N. C. Cady, C. A. Batt, G. G. Malliaras, *Chem. Commun.* **2004**, 1556; b) F. Yan, S. M. Mok, J. Yu, H. L. Chan, M. Yang, *Biosensors Bioelectron.* **2009**, *24*, 1241; c) G. Tarabella, G. Nanda, M. Villani, N. Coppede, R. Mosca, G. G. Malliaras, C. Santato, S. Iannotta, F. Cicoira, *Chem. Sci.* **2012**, *3*, 3432.
[9] M. H. Bolin, K. Svennersten, D. Nilsson, A. Sawatdee, E. W. Jager, A. Richter-Dahlfors, M. Berggren, *Adv. Mater.* **2009**, *21*, 4379.
[10] P. Lin, F. Yan, J. Yu, H. L. Chan, M. Yang, *Adv. Mater.* **2010**, *22*, 3655.
[11] L. H. Jimison, S. A. Tria, D. Khodagholy, M. Gurfinkel, E. Lanzarini, A. Hama, G. G. Malliaras, R. M. Owens, *Adv. Mater.* **2012**.
[12] D. Khodagholy, T. Doublet, P. Quilichini, M. Gurfinkel, P. Leleux, A. Ghestem, E. Ismailova, T. Herve, S. Sanaur, C. Bernard, *Nature Communications* **2013**, *4*, 1575.
[13] H. S. White, G. P. Kittlesen, M. S. Wrighton, *J. Am. Chem. Soc.* **1984**, *106*, 5375.
[14] S. Kirchmeyer, A. Elschner, K. Reuter, W. Lovenich, *PEDOT as a Conductive Polymer: Principles and Applications*, CRC, **2010**.
[15] Y. Xia, C. D. Frisbie, *Organic Electronics II* **2012**, *6*, 1.
[16] a) K. Pernstich, S. Haas, D. Oberhoff, C. Goldmann, D. Gundlach, B. Batlogg, A. Rashid, G. Schitter, *J. Appl. Phys.* **2004**, *96*, 6431; b) F. Maddalena, E. Meijer, K. Asadi, D. de Leeuw, P. Blom, *Appl. Phys. Lett.* **2010**, *97*, 043302.
[17] L. Kergoat, L. Herlogsson, B. Piro, M. C. Pham, G. Horowitz, X. Crispin, M. Berggren, *Proceedings of the National Academy of Sciences* **2012**, *109*, 8394.
[18] G. Tarabella, C. Santato, S. Y. Yang, S. Iannotta, G. G. Malliaras, F. Cicoira, *Appl. Phys. Lett.* **2010**, *97*, 123304.
[19] D. Khodagholy, M. Gurfinkel, E. Stavrinidou, P. Leleux, T. Herve, S. Sanaur, G. G. Malliaras, *Appl. Phys. Lett.* **2011**, *99*, 163304.
[20] D. A. Bernards, D. J. Macaya, M. Nikolou, J. A. DeFranco, S. Takamatsu, G. G. Malliaras, *J. Mater. Chem.* **2007**, *18*, 116.
[21] M. Sessolo, D. Khodagholy, J. Rivnay, F. Maddalena, M. Gleyzes, E. Steidl, B. Buisson, G. G. Malliaras, *Adv. Mater.* **2013**, *25*, 2135.
[22] D. Khodagholy, J. Rivnay, M. Sessolo, M. Gurfinkel, P. Leleux, L. H. Jimison, E. Stavrinidou, T. Herve, S. Sanaur, R. M. Owens, G. G. Malliaras, *Nature Communications* **2013**, *4*, 2133.